Am J Transl Res 2017;9(4):1680-1693
www.ajtr.org /ISSN:1943-8141/AJTR0043237

Original Article

Effects of altered CXCL12/CXCR4 axis on BMP2/Smad/Runx2/Osterix axis and osteogenic gene expressions during osteogenic differentiation of MSCs

Zhanghua Li[1], Wei Wang[2], Haijia Xu[1], Yu Ning[2], Weijun Fang[3], Wen Liao[1], Ji Zou[2], Yi Yang[4], Ningsheng Shao[5]

[1]Tongren Hospital of Wuhan University, Wuhan 430060, Hubei, China; [2]Hubei University of Chinese Medicine, Wuhan 430065, Hubei, China; [3]Renmin Hospital of Wuhan University, Wuhan 430060, Hubei, China; [4]Health Science College, Wuhan Sports University, Wuhan 430079, China; [5]Department of Biochemistry and Molecular Biology, Institute of Basic Medical Sciences, Academy of Military Medical Sciences, Beijing 100000, China

Received October 31, 2016; Accepted March 21, 2017; Epub April 15, 2017; Published April 30, 2017

Abstract: This study investigated the effects of altered CXCL12/CXCR4 axis on the bone morphogenetic protein 2 (BMP-2)/Smad/runt-related transcription factor 2 (Runx2)/Osterix (Osx) signal axis and osteogenic gene expression during osteogenic differentiation of mesenchymal stem cells (MSCs), to gain understanding of the link between migration and osteogenic differentiation signal axis and MSCs osteogenic differentiation mechanisms. The pHBAd-MCMV-CXCL12-GFP vector (Ad-CXCL12) was constructed and quantitative polymerase chain reaction (qPCR)/western blotting used to determine CXCL12 expression in Ad-CXCL12-transfected MSCs. MSCs were treated with Ad-CXCL12 and AMD3100 (CXCL12 inhibitor) to detect BMP-2/Smad/Runx2/Osterix expression, bone sialoprotein (BSP), osteocalcin (OCN) and osteopontin (OPN) mRNA expression, and alkaline phosphatase (ALP) activity. PCR and sequencing confirmed successful construction of Ad-CXCL12. qPCR and enzyme-linked immunosorbent assay indicated that Ad-CXCL12 transfection promoted CXCL12 expression in MSCs. At 72 hours, Runx2 and Osterix, and Smad1/5/8 mRNA and protein expressions were significantly higher in the Ad-CXCL12 group than in the control group ($P < 0.01$). At 1 and 2 weeks, ALP activity and BSP mRNA expression were significantly higher in the Ad-CXCL12 group than in the control group ($P < 0.01$), respectively. No significant difference in *OCN* and *OPN* mRNA expression was determined between Ad-CXCL12 and control groups ($P > 0.05$). At 3 weeks, no significant difference in mineralized nodule staining was observed between groups ($P > 0.05$). Changes in the CXCL12/CXCR4 migration axis affected the BMP-2/Smad/Runx2/Osterix axis and *BSP*, *OCN* and *OPN* mRNA expression in early-stage, but not mid-/late-stage, MSCs osteogenic differentiation, therefore affecting the ability of MSCs to undergo osteogenic differentiation.

Keywords: Gene transfection, mesenchymal stem cells (MSCs), osteogenic gene, osteogenic differentiation, cell migration, c-x-c motif chemokine ligand 12 (CXCL12)

Introduction

Avascular necrosis of the femoral head (ANFH) is a highly debilitating disease. Patients tend to choose artificial hip replacement due to hip pain and limited mobility after collapse and deformation of the femoral head. However, current non-surgical and surgical methods used in the treatment of ANFH have limitations. Given their strong self-renewal and multi-lineage differentiation potentials, mesenchymal stem cells (MSCs) can migrate to sites of injury and repair tissues after *in vivo* transplantation [1]. Previous studies [2-4] have used experimental and clinical approaches to assess the use of MSCs for treating ANFH, however the results have been unsatisfactory to date. The reasons for this may include: (1) insufficient homing of MSCs after transplantation; and (2) weak osteogenic differentiation of the MSCs after homing. One *in vivo* study using MSCs demonstrated a low rate of homing at the injury site after their injection [5]. It has been reported that the hypoxic environment at the site of injury weakens the ability of MSCs to undergo osteogenic differentiation by suppressing calcium nodule formation and extracellular calcium salt deposition, downregulating osteogenic gene (*BMP-2*

and *Runx2*) expression, and inhibiting the growth and differentiation of osteoblasts and thus impacting bone formation [6, 7]. Identifying methods to better promote MSCs differentiation into osteoblasts and improve their homing ability is therefore critical for their clinical application.

The c-x-c motif chemokine ligand 12 (CXCL12) and its CXCR4 receptor form the CXCL12/CXCR4 axis, which is most strongly associated with cell migration. The CXCL12/CXCR4 axis promotes stem cell homing to the injured area along a concentration gradient, and participates in the repair of tissues and organs [8]. CXCL12 is a small protein that belongs to the chemokine family. CXCL12 binding to seven-transmembrane G protein-coupled receptor CXCR4 is extensively involved in stem cell homing [9], tissue repair [10], immunoregulation [11], and tumor cell migration [12]. After the occurrence of ANFH, hypoxia-inducible factor-1α, an important transcription factor in the regulation of hypoxia in animals, can be blocked during the decomposition and quickly accumulates at the site [13], activating the expression of more than 60 downstream target genes, including CXCL12 [14]. Furthermore, CXCL12 contributes to vascular endothelial growth factor (VEGF) expression in vascular endothelial cells and inhibition of the CXCL12/CXCR4 axis suppresses VEGF-dependent angiogenesis [15]. The CXCL12/CXCR4 axis has specific effects on osteogenic differentiation of MSCs. Hosogane et al. [16] found that when CXCL12 or CXCR4 expression was blocked, MSCs osteogenic differentiation was inhibited in bone morphogenetic protein 2 (BMP-2)-medicated mice. Additionally, Zhu et al. [17] found that CXCL12 promoted BMP-2-induced osteogenic differentiation of C2C12 cells. These findings suggest that CXCL12 is not only strongly associated with MSCs homing, but also participates directly in their osteogenic differentiation. To verify this in the present study, an adenovirus vector carrying the *CXCL12* gene was constructed *in vitro* to promote *CXCL12* gene overexpression in MSCs, and the CXCL12 inhibitor AMD3100 was used to inhibit *CXCL12* mRNA expression. This study aimed to determine the effects of the CXCL12/CXCR4 axis in the activated or inhibited state on the BMP-2/Smad/Runx2/Osterix signal axis and osteogenic gene (*BSP*, *OCN* and *OPN*) expression during MSCs osteogenic differentiation. The findings will aid our understanding of the intrinsic link between the migration and osteogenic differentiation signal axes, and MSCs osteogenic differentiation mechanisms, thus providing a strong experimental basis for stem cell gene therapy for ANFH.

Materials and methods

Materials

Materials used in this study included pHBAd-MCMV-GFP vector (Hanbio Biotechnology Co., Ltd., Shanghai, China), E. coli strain DH5α (Tiangen Biotech (Beijing) Co., Ltd., China), restriction enzyme, T4 ligase and DNA ladder (Fermentas, Canada), Plasmid DNA Extraction Kit (CWBIO Biotechnology Co., Ltd., Beijing, China), Gel Recovery Kit (Axygen, USA), agarose, agar powder (Biowest, France), human embryonic kidney cell line HEK293 cells and MSCs (gifted by Laboratory of Biochemistry and Molecular Biology, Institute of Basic Medicine, Academy of Military Medical Sciences), Dulbecco's Modified Eagle's Medium (DMEM), fetal bovine serum (FBS) and trypsin (Hyclone, USA), glutamine, sodium β-glycerophosphate (Sigma, USA), double antibody, CXCL12 inhibitor AMD3100 (Invitrogen, USA), membrane filter (Millipore), ALP Detection Kit (NanJingJianCheng Bioengineering Institute, China), Runx2 rabbit polyclonal antibody (LSBio, USA), Osterix rabbit polyclonal antibody, BMP-2 mouse monoclonal antibody (Abcam, USA), Smad1/5/8 rabbit polyclonal antibody (Santa Cruz Biotechnology, USA), primers (synthesized by Sangon Biotech (Shanghai) Co., Ltd., China), 0.1% alizarin red S stain, and 4% paraformaldehyde (Beijing Leagene Biotechnology Co., Ltd., China).

Construction and identification of CXCL12 adenovirus expression vector

Synthetic CXCL12 target genes were amplified by PCR. The pHBAd-MCMV-GFP vector was digested with ECORI and SmaI followed by gel recovery, and the target gene fragment was ligated with the vector. The ligation product was transferred into E. coli strain DH5α competent cells using the heat shock method and seeded in Amp agar plates at 37°C overnight. After transformation, the bacteria were picked and shaken at 250 rpm and 37°C for 14 hours. The bacteria in the solution were then identified by

Table 1 Gene primer sequences

Gene name	Upstream primer (5'-3')	Downstream primer (3'-5')
GAPDH	TGG AAT CCA CTG GCG TCT TC	GGT TCA CGC CCA TCA CAA AC
CXCL12	CTC TGC ATC AGT GAC GGT AAG C	AAT CTG AAG GGC ACA GTT TGG
BMP-2	TGT GGA CTT CAG TGA TGT G	TGG AGT TCA GGT GGT CAG
Smad1	CTC ATG TCA TTT ATT GCC GTG TG	CGC TTA TAG TGG TAG GGG TTG A
Smad5	TGC CTA TAT GCC ACC TGA T	CTG AAC ATC TCT GCT GGA TAT
Smad8	CGG GTC AGC CTA GCA AGT G	GTG CCG AAC GGG AAC TCA C
Runx2	GAC TGT GGT TAC CGT CAT GGC	ACT TGG TTT TTC ATA ACA GCG GA
Osterix	TCC CTG GAT ATG ACT CAT CCC T	CCA AGG AGT AGG TGT GTT GCC
BSP	TTT TGG GAA AAC CAC TGC CG	TCG GTA ATT GTC CCC ACG AG
OCN	CTC CTT ACC CGG ATC CCC TG	GTA GAA GCG CTG GTA GGC GT
OPN	TCC AAA GTC AGC CAG GAA TCC	CGG AGT TGT CTG TGC TCT TCA

polymerase chain reaction (PCR). Positive clones were sequenced by Shanghai Sunny Biotechnology Co., Ltd., China. The bacterial solution (2 mL) in logarithmic phase was added to 100 mL of LB medium containing 100 μg/mL Amp, and shaken at 300 rpm and 37°C overnight. After the plasmid was extracted, the 293T cells were incubated in a 60 mm Petri dish. When the cells reached 70-80% confluence, the CXCL12 recombinant adenovirus vector plasmid and backbone plasmid (pBAd-BHG) were transfected with Lipofiter™ transfection reagent. Signs of cell infection were observed daily. When the majority of cells displayed signs of infection and lost adherence, the viruses were collected as follows. All cells and medium from the 60 mm Petri dish were placed in a 15-mL centrifuge tube for freeze-thawing three times, followed by centrifugation at 3000 rpm for 5 minutes. The supernatant was collected and labeled as the first generation of virus (P1) and the cells were repeatedly infected with P1. The virus was collected as previously described, and after filtration and purification, the titer was determined. All samples were stored individually at -70°C.

CXCL12 mRNA expression after MSCs transfection with CXCL12 recombinant adenovirus

MSCs were incubated in six-well plates at a density of 2 × 10^5 cells/well. At 80% confluence, the MSCs were incubated in serum-free medium supplemented with Ad-CXCL12 (multiplicity of infection = 60). MSCs alone were used as the control group. MSCs were further incubated at 37°C, 5% CO_2 and 100% humidity for 6 hours, then incubated in L-glutamine-containing DMEM (L-DMEM) containing 10% FBS for 72 hours prior to harvesting. Trizol lysate (1 mL) was added to each well and total RNA was extracted. RNA (1 μg) was reverse transcribed and examined by quantitative polymerase chain reaction (qPCR). Each gene sequence was searched in the National Center for Biotechnology Information (NCBI) database. Primers were designed with Premier5 software. All primers were synthesized by Sangon Biotech Co. Ltd. (Shanghai, China) and all primer sequences are listed in **Table 1**. The reaction included 10 μL of 2 × UltraSYBR Mixture, 1 μL of upstream primer, 1 μL of downstream primer, and 1 μL of cDNA, with ddH_2O added to a total volume of 20 μL. Reaction conditions were as follows: initial denaturation at 95°C for 10 minutes, 40 cycles of denaturation at 95°C for 15 seconds, annealing at 60°C for 30 seconds, and extension at 60°C for 30 seconds. Glyceraldehyde 3-phosphate dehydrogenase (GAPDH) was used as an internal reference and each experiment was performed in triplicate.

Detection of CXCL12 contents in the supernatant after MSCs transfection with CXCL12 recombinant adenovirus

MSCs were incubated in six-well plates at a density of 2 × 10^5 cells/well. At 80% confluence, MSCs were incubated with serum-free medium supplemented with Ad-CXCL12 (multiplicity of infection = 60). MSCs alone were used as the control group. MSCs were further incubated at 37°C, 5% CO_2 and 100% humidity for 72 hours, and then centrifuged at 3000 rpm for 15 minutes. After the supernatant was obtained, CXCL12 protein content was determined using a double-antibody sandwich enzyme-linked immunosorbent assay (ELISA). Supernatant and standard products were diluted to different concentrations and added (50 μL/well) to the ELISA plate pre-coated with antibody. Except for the blank well, 100 μL of horseradish peroxidase-labeled secondary antibody

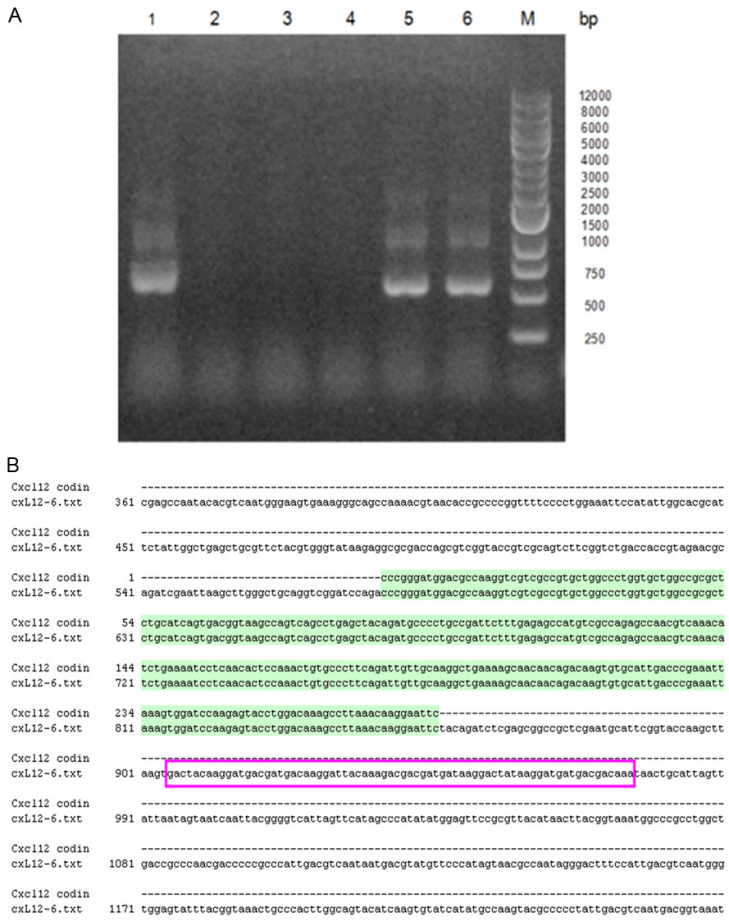

Figure 1. Monoclone and gene sequencing by PCR. A: PCR results of monoclone. 1-6: monoclones; M: GeneRay 1 kb DNA Marker. The constructed vector was approximately 600 bp. Electrophoresis results demonstrated the bands at 500-750 bp in lanes 1, 5 and 6. The bacteria solution with positive bands was sequenced. B: Gene sequencing results. Green represents *CXCL12* gene; purple box shows 3× flag sequence. Sequencing reveal that the *CXCL12* gene had inserted into the plasmid. The 3× flag sequence in the purple box is the sequence carried by the vector.

was added to each well and the plate was incubated at 37°C for 1 hour. After removal of the reaction solution, the samples were dried on absorbent paper and washed three times with buffer solution. After air-drying, substrates A and B (each 50 μL) were added to each well and the plate was incubated at 37°C in the dark for 15 minutes. The reaction was terminated by adding 50 μL of stop solution to each well and absorbance values were measured at 450 nm on a microplate reader. CXCL12 contents in the supernatant of each group were calculated in accordance with standard curve. Average values were calculated from three measurements of each sample.

MSCs culture and group assignment

MSCs were incubated with L-DMEM supplemented with 10% FBS, 100 U/mL penicillin and 100 g/mL streptomycin at 37°C, 5% CO_2 and 100% humidity. The medium was replaced every two or three days. At 80% confluence, the cells were digested with 0.25% trypsin and were randomly divided into control group, negative control group (Ad-GFP), AMD-3100 group, CXCL12 gene overexpression group (Ad-CXCL12), and ADM3100+CXCL12 gene overexpression group (Ad-CXCL12+AMD3100). At 80% confluence, Ad-GFP (multiplicity of infection = 60) was added in the Ad-GFP group; and Ad-CXCL12 (multiplicity of infection = 60) was added in the Ad-CXCL12 and Ad-CXCL12+ AMD3100 groups. Six hours later, MSCs were incubated with osteogenic induction medium containing H-DMEM, 10% FBS, 10^{-8} mol/L dexamethasone, 10 mmol/L sodium β-glycerophosphate, 50 μg/mL vitamin C, and 2 mmol/L glutamine. Finally, 50 μmol/L AMD3100 was added in the AMD3100 and Ad-CXCL12+AMD3100 groups.

qPCR detection of BMP-2, Smad1/5/8, Runx2 and Osterix mRNA expressions

After 72 hours of treatment, cells from each group were harvested. Trizol lysate (1 mL) was added to each well. Total RNA was extracted and the concentration measured. RNA (1 μg) was reverse transcribed and examined with qPCR. The corresponding gene sequence was searched in the NCBI database and primers were designed with Premier5 software. The primer sequences are shown in **Table 1**. The reaction included 10 μL of 2 × UltraSYBR Mixture, 1 μL of upstream primer, 1 μL of downstream primer, and 1 μL of cDNA, with ddH_2O

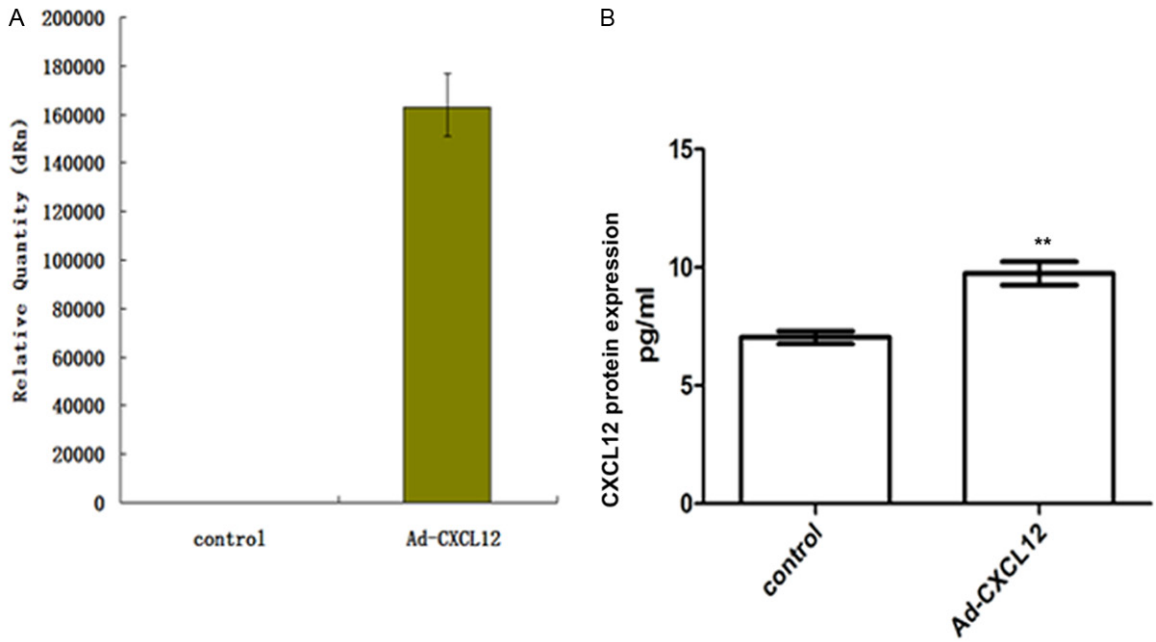

Figure 2. *CXCL12* mRNA and protein expression after MSCs transfection with Ad-CXCL12. A: *CXCL12* mRNA expression after MSCs were transfected with Ad-CXCL12 as detected by qPCR. At 72 hours after transfection with Ad-CXCL12, *CXCL12* mRNA expression was significantly higher in the transfected group than in the non-transfected group. B: CXCL12 content in the supernatant after MSCs were transfected with Ad-CXCL12 as measured by ELISA. CXCL12 content was significantly higher in the supernatant from the transfected group than in the non-transfected group (**$P \leq 0.01$).

added to a total volume of 20 μL. Reaction conditions were as follows: initial denaturation at 95°C for 10 minutes, 40 cycles of denaturation at 95°C for 15 seconds, annealing at 60°C for 30 seconds, and extension at 60°C for 30 seconds. GAPDH was used as an internal reference and each experiment was performed in triplicate.

Western blotting for Smad1/5/8, Runx2 and Osterix protein expression

After 72 hours of treatment, MSCs in each group were harvested and washed twice with PBS. The MSCs were then incubated with precooled protein extraction reagent containing protease inhibitors (50 μL of extraction reagent per 1 × 10^6 cells) in an iced bath at room temperature for 30 minutes, then centrifuged at 12000 rpm and 4°C for 15 minutes. The supernatant was obtained and the concentration of protein in the samples determined by the bicinchoninic acid assay. The supernatant was then denatured in protein buffer at 100°C for 10 minutes and proteins were separated by sodium dodecyl sulfate-polyacrylamide gel electrophoresis. Following electrophoresis, the proteins were transferred onto polyvinylidene fluoride membranes at 80 V for 80 minutes. Membranes were blocked with 5% non-fat dry milk for 1 hour, and incubated with antibodies (primary antibody and horseradish peroxidase-labeled secondary antibody). The blots were visualized with the chemiluminescence detection kit (Thermo Fisher Scientific). The labeled bands were visualized and quantified using a chemiluminescence imaging system (CliNX, Shanghai, China). GAPDH served as an internal reference and experiments were conducted in triplicate.

Detection of ALP activity

After one week of treatment, MSCs in each group were harvested and washed twice with PBS. The MSCs were then incubated with precooled protein extraction reagent containing protease inhibitors (50 μL of extraction reagent per 1 × 10^6 cells) in an iced bath at room temperature for 30 minutes, and centrifuged at 12000 rpm and 4°C for 15 minutes. The supernatant was obtained and the concentration of protein in the samples was determined by the bicinchoninic acid assay. In accordance with

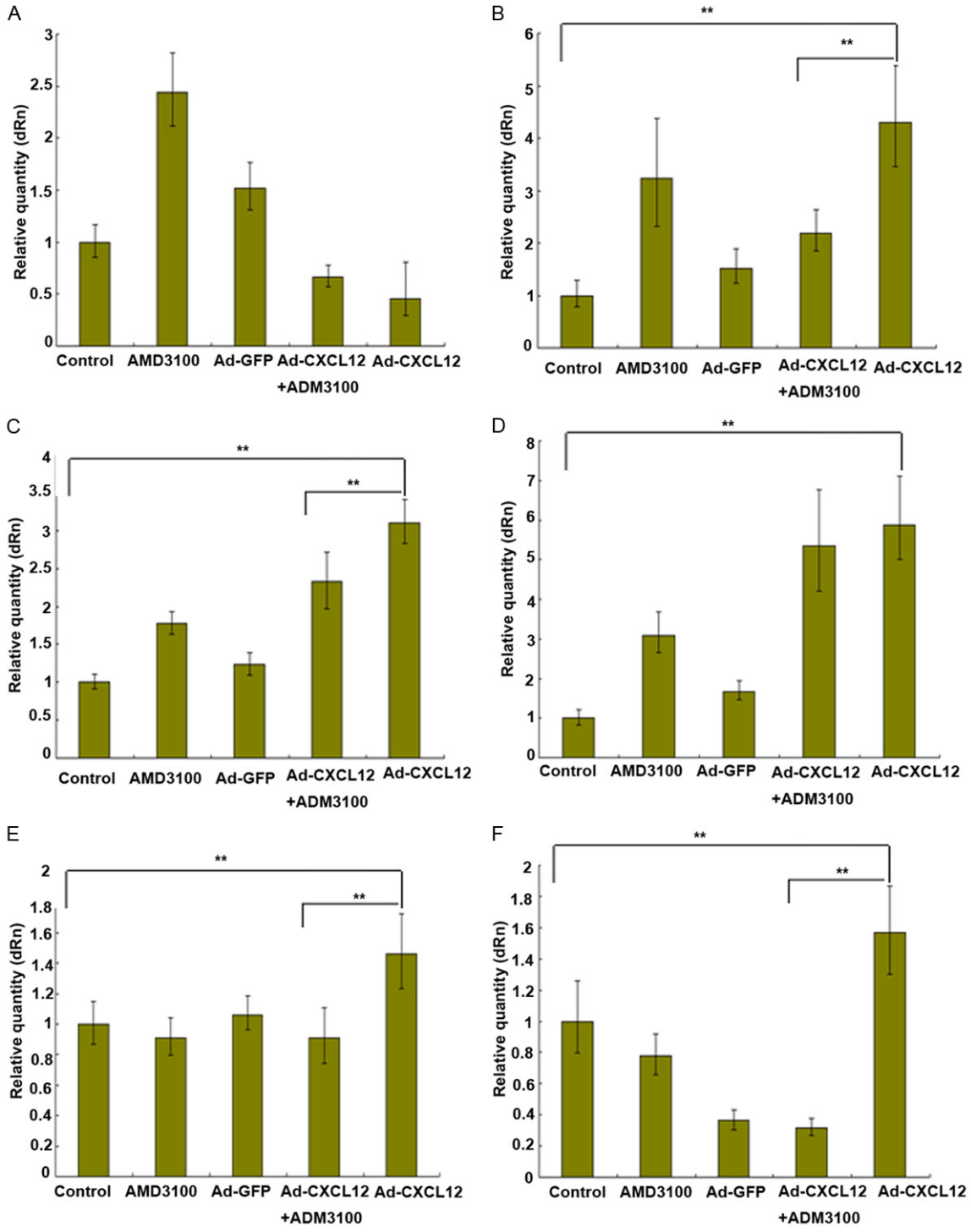

Figure 3. Gene expressions 72 hours after MSCs transfection with CXCL12. mRNA expression of (A) *BMP-2*; (B) *Smad1*; (C) *Smad5*; (D) *Smad8*; (E) *Runx2*; and (F) *Osterix*. At 72 hours after transfection, *BMP-2* mRNA expression was not significantly increased in the Ad-CXCL12 group compared with the control group. However, *Smad1/5*, *Runx2* and *Osterix* mRNA expressions were significantly higher in the Ad-CXCL12 group than in the control and Ad-CXCL12+AMD3100 groups (**P ≤ 0.01). *Smad8* mRNA expression was significantly higher in the Ad-CXCL12 group than in the control group (**P ≤ 0.01).

the ALP detection kit instructions, absorbance values in each well were measured at 510 nm with a microplatereader. ALP activity was equal to $(OD_{detection}\text{-}OD_{blank})/(OD_{standard}\text{-}OD_{blank})$ × stan-

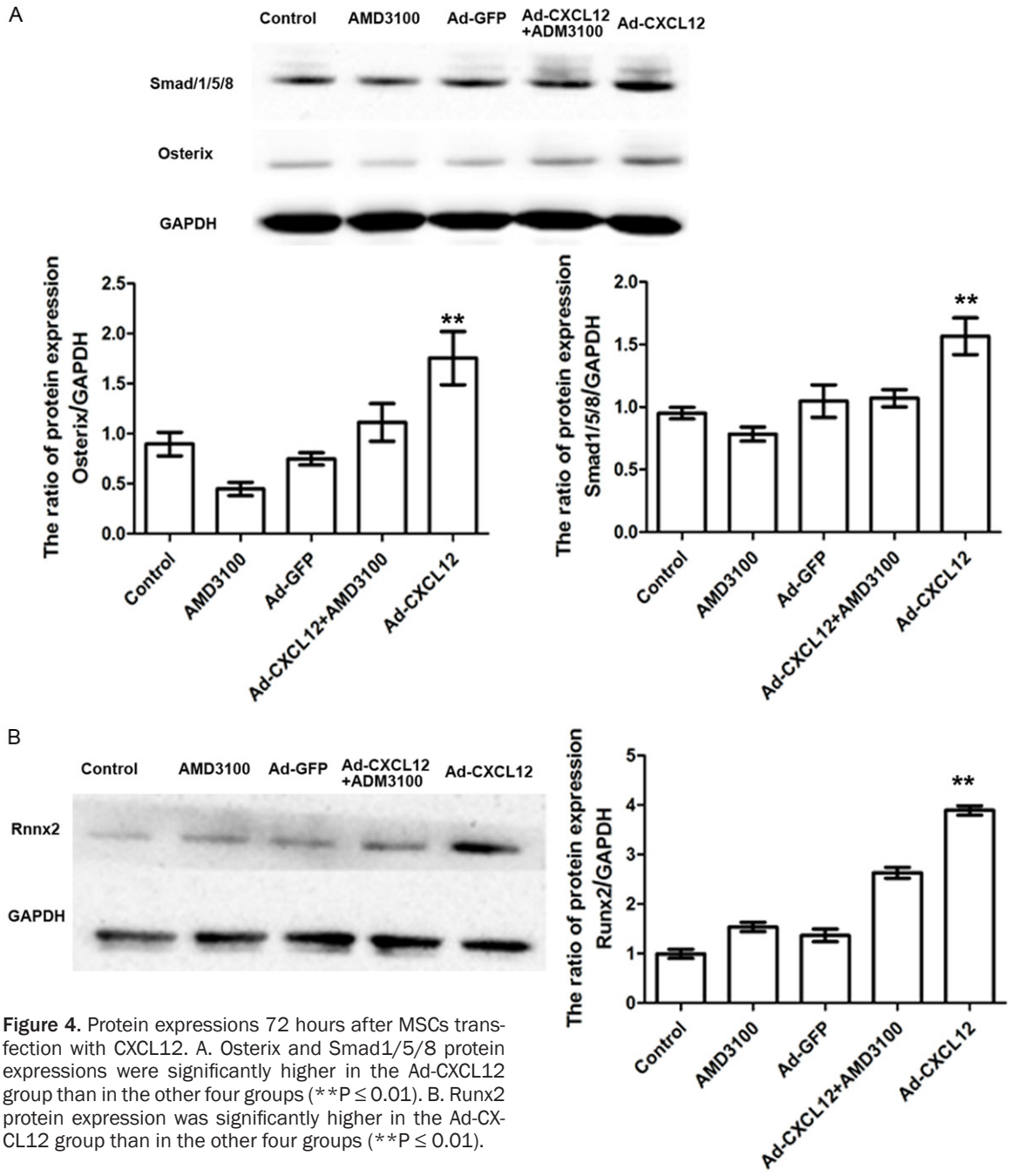

Figure 4. Protein expressions 72 hours after MSCs transfection with CXCL12. A. Osterix and Smad1/5/8 protein expressions were significantly higher in the Ad-CXCL12 group than in the other four groups (**P ≤ 0.01). B. Runx2 protein expression was significantly higher in the Ad-CXCL12 group than in the other four groups (**P ≤ 0.01).

dard concentration (0.1 mg/mL)/protein concentration$_{measured}$ (gprot/mL). Average values were calculated from three measurements of each sample and experiments were conducted in triplicate.

qPCR detection of BSP, OCN and OPN mRNA expressions

After two weeks of treatment, MSCs in each group were harvested. Briefly, Trizol lysate (1 mL) was added to each well. Total RNA was extracted and the concentration was measured. RNA (1 μg) was reverse transcribed and examined with qPCR. Each gene sequence was searched in the NCBI database. Primers were designed with Premier5 software and primer sequences are shown in **Table 1**. The reaction included 10 μL of 2 × UltraSYBR Mixture, 1 μL of upstream primer, 1 μL of downstream primer, and 1 μL of cDNA, with ddH_2O added to a total volume of 20 μL. Reaction conditions were

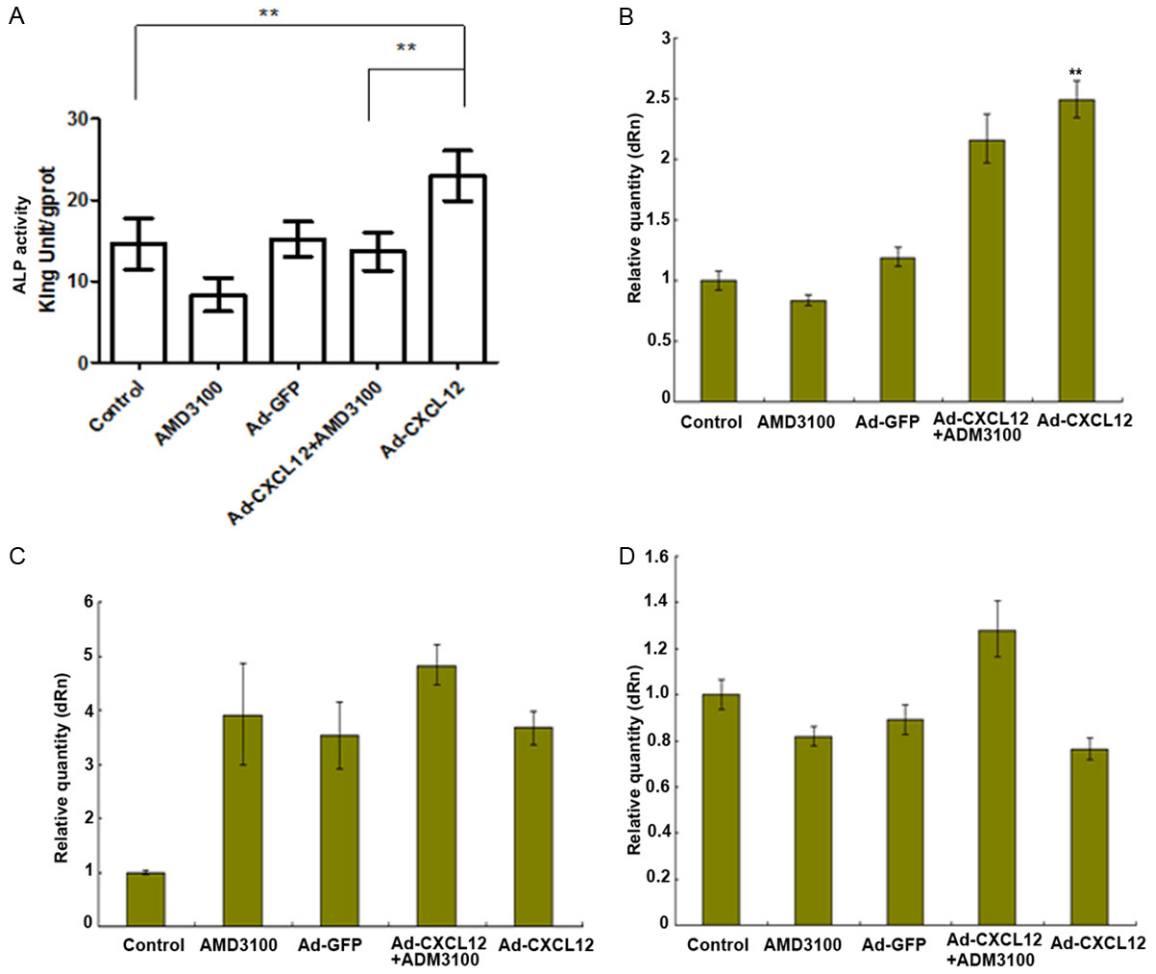

Figure 5. ALP activity and *BSP*, *OCN* and *OPN* mRNA expressions after MSCs transfection with CXCL12. A: ALP expression one week after MSCs were transfected with CXCL12. ALP activity was significantly higher in the Ad-CXCL12 group than in the control and Ad-CXCL12+AMD3100 groups (**P ≤ 0.01); B: *BSP* mRNA expression two weeks after MSCs were transfected with CXCL12 (**P ≤ 0.01, vs. control group and Ad-GFP group). C: *OCN* mRNA expression two weeks after MSCs were transfected with CXCL12. No significant difference in *OCN* mRNA expression was observed between Ad-CXCL12 and Ad-GFP groups (P = 0.216 > 0.05). D: *OPN* mRNA expression two weeks after MSCs were transfected with CXCL12. *OPN* mRNA expression was not significantly increased in the Ad-CXCL12 group compared with the control group.

as follows: initial denaturation at 95°C for 10 minutes, 40 cycles of denaturation at 95°C for 15 seconds, annealing at 60°C for 30 seconds, and extension at 60°C for 30 seconds. GAPDH was used as an internal reference and each experiment was performed in triplicate.

Determination of mineralized nodules

Three weeks after culture, MSCs were stained with Alizarin Red S. Briefly, after removal of the medium, MSCs were washed three times with PBS, fixed with 4% paraformaldehyde for 15 minutes, washed three times with ddH_2O, and stained with 0.1% Alizarin Red S (pH 8.3). When accumulated orange-red matter was visualized, the staining solution was removed by absorbing onto a paper towel. After three washes with ddH_2O, the samples were observed and photographed with Laika DM1000 microscope (Laika, German) and attached camera. Cetylpyridinium chloride (10%) was added to each well (1 mL) to dissolve the dye from the mineralized nodules. The absorbance values in each well were measured at 490 nm with a microplate reader. Cetylpyridinium chloride-only (10%) was used for zero adjustment. Each experiment was performed in triplicate.

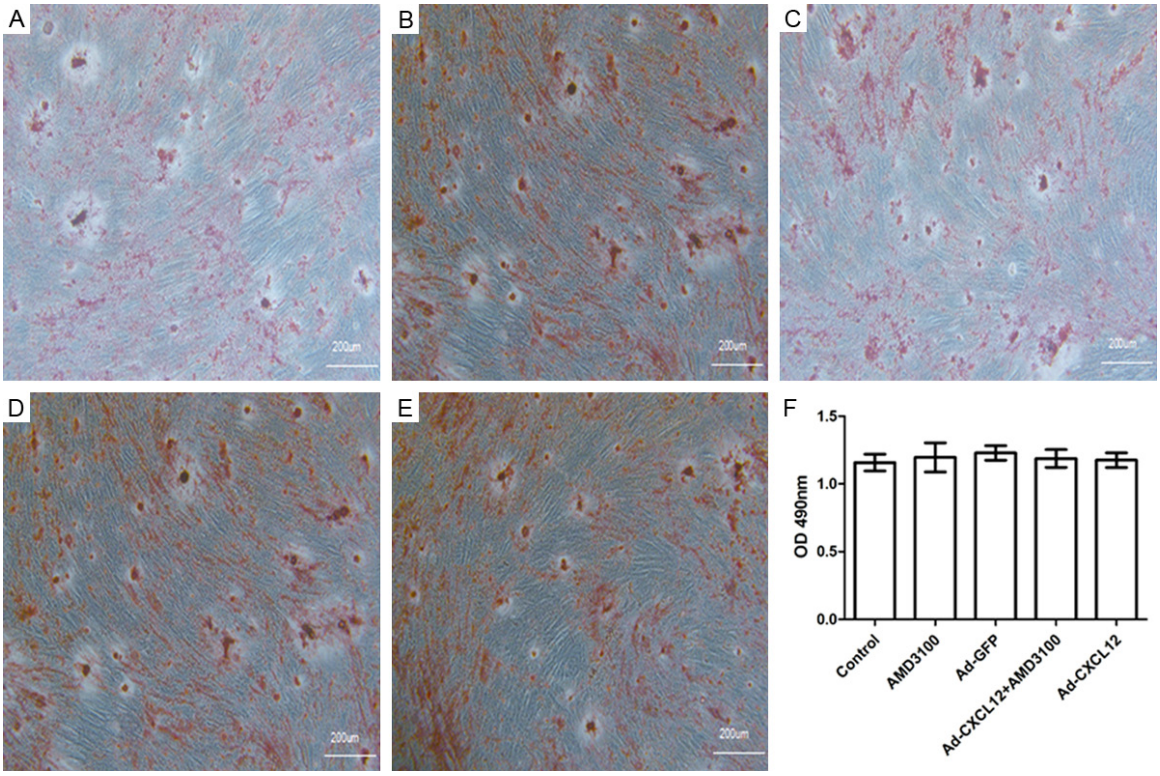

Figure 6. Alizarin red staining and quantification of mineralized nodules three weeks after MSCs transfection. Photomicrographs of alizarin red-stained MSCs in: A. Control; B. AMD3100; C. Ad-GFP; D. Ad-CXCL12+AMD3100; and E. Ad-CXCL12 groups. After photographing, mineralized nodules were dissolved with 10% cetylpyridinium chloride and the absorbance values measured at 490 nm. F. No significant differences in absorbance values were observed among groups.

Statistical analysis

All data were expressed as the means ± standard deviation (SD), and analyzed with SPSS 16.0 software. One-way analysis of variance (ANOVA) was used to compare the differences among groups. A value of $P < 0.05$ was considered statistically significant.

Results

pHBAd-MCMV-GFP vector identification and sequencing

After transfection with CXCL12, PCR results revealed positive clones in lanes 1, 5 and 6 (**Figure 1A**). Electrophoresis results displayed that CXCL12 was completely inserted into the plasmid (**Figure 1B**).

Detection of CXCL12 mRNA and protein expressions after MSCs transfected with Ad-CXCL12

At 72 hours after transfection with Ad-CXCL12, qPCR and ELISA demonstrated that CXCL12 mRNA expression was significantly higher in the Ad-CXCL12 group than in the non-transfected group ($P \leq 0.01$; **Figure 2A**). Furthermore, CXCL12 protein expression was significantly higher in the Ad-CXCL12 group than in the control group ($P \leq 0.01$; **Figure 2B**). These results suggested that exogenous CXCL12 could enhance CXCL12 expression in MSCs, and further verified the success of Ad-CXCL12 construction.

BMP-2, Smad1/5/8, Runx2, and Osterix mRNA expression determined by qPCR

BMP-2, Smad1/5/8, Runx2, and Osterix mRNA expression levels 72 hours after Ad-CXCL12 transfection are shown in **Figure 3**. Smad1/5/8, Runx2 and Osterix mRNA expression levels were greater in the Ad-CXCL12 group than in the control group ($P \leq 0.01$). Furthermore, Smad1, Smad5, Runx2, and Osterix mRNA expression levels were significantly lower in the Ad-CXCL12+AMD3100 group than in the Ad-CXCL12 group ($P \leq 0.01$), however BMP-2 mRNA expression was not increased in the Ad-CXCL12 group.

Western blotting for Smad1/5/8, Runx2 and Osterix protein expression

At 72 hours after transfection with Ad-CXCL12, cells were harvested and total protein was extracted. Western blotting showed that Smad1/5/8, Runx2 and Osterix protein expression levels were significantly higher in the Ad-CXCL12 group than in the control group. Gray value analysis found that the relative gray values of Smad1/5/8, Runx2 and Osterix were higher in the Ad-CXCL12 group than in the other four groups (**P < 0.01). These results indicated that Ad-CXCL12 transfection contributed to Smad1/5/8, Runx2 and Osterix mRNA expression in the signal axis, and AMD3100 decreased these effects (**Figure 4**).

Detection of ALP activity and BSP, OCN and OPN mRNA expressions

One week after transfection, ALP activity within the total protein was determined in each group (**Figure 5A**). ALP activity was significantly higher in the Ad-CXCL12 group than in the control group ($P \leq 0.01$) and was significantly decreased after treatment with AMD3100 ($P \leq 0.01$). These results suggested that exogenous CXCL12 enhanced ALP expression in MSCs. Two weeks after transfection, BSP mRNA expression was significantly higher in the Ad-CXCL12 group than in the control and Ad-GFP groups ($P \leq 0.01$). However, no significant difference in OCN mRNA expression was detected between the Ad-CXCL12 and Ad-GFP groups ($P = 0.216 > 0.05$). Similarly, OPN mRNA expression was not increased in the Ad-CXCL12 group compared with the control and Ad-GFP groups (**Figure 5B-D**).

Mineralized nodule formation

Three weeks after transfection, alizarin red staining did not reveal any significant differences in the numbers of mineralized nodules among groups. Furthermore, after the mineralized nodules were dissolved with 10% cetylpyridinium chloride, no significant differences in absorbance values at 490 nm were determined among groups. These results suggest that the overexpression or inhibition of CXCL12 expression had no significant effect on the late stage of osteogenic differentiation of MSCs (**Figure 6**).

Discussion

Chemokines are classified into four classes according to their molecular structure: CXC, CX3C, CC, and C, with CXCL12 belonging to the CXC subfamily [18]. CXCL12 and its G protein-coupled receptor CXCR4 are extensively expressed in various tissues. Increasing evidence suggests that the CXCL12/CXCR4 signal axis is strongly associated with MSCs tissue repair in muscle [19], kidney [20], heart [21], liver [22], and bone [23]. It is believed that the CXCL12/CXCR4 axis guides MSCs homing to the injured area [25], thus increasing the number of MSCs and their participation in angiogenesis at the injury site [26]. Regarding the effects of CXCL12 on bone injury, Chen et al. [24] found that local injection of CXCL12 promoted the repair of bone nonunion with MSCs. To further verify whether the CXCL12/CXCR4 axis can directly regulate MSCs osteogenic differentiation, this study constructed an adenovirus vector carrying the CXCL12 gene for MSCs transfection, and observed changes in the BMP-2/Smads/Runx2/Osterix signal axis and osteogenic gene expression after CXCL12/CXCR4 axis activation or inhibition. Furthermore, difference in the number of mineralized nodules among groups was determined. This study aimed to provide a reliable experimental basis for our hypothesis that CXCL12/CXCR4 axis not only promotes MSCs homing, but also contributes to osteogenic differentiation of MSCs.

The BMP-2/Smads/Runx2/Osterix axis is a key signal axis that regulates the differentiation of MSCs into osteoblasts [27]. BMP-2 has a strong promoting effect on osteogenic differentiation and is one of the most widely studied BMPs. BMP-2 contributes to Runx2 mRNA expression by activating Smads (Smad1, Smad5 and Smad8). Runx2 is a specific osteogenic transcription factor, expressed relatively early during MSCs osteogenic differentiation [28]. Runx2 is the most specific gene expressed during osteogenesis [28]. Its DNA-binding site is located in the promoter region of many osteoblast-specific genes. Runx2 regulates gene transcription after binding to effector elements on these promoters. The level of functional Runx2 determines the degree of bone maturation and conversion rate [29]. Our previous studies have shown that changes of Runx2 mRNA expression in the necrotic femoral head of VFHN patients occurred earlier than the

imaging and morphological changes, and continued to increase, indicating that bone remodeling begins in the early-stage of VFHN, and that the Runx2 gene participates and regulates this process [30]. Osterix, a downstream signaling gene of Runx2, is an essential transcription factor in osteoblast differentiation [31]. Consequently, Runx2/Osterix is often considered as a marker for early osteogenic differentiation. In this study, Smad1/5/8, Runx2 and Osterix mRNA and protein expressions were dramatically higher in the Ad-CXCL12 group than in the non-transfected group, but were diminished in the Ad-CXCL12+AMD3100 group. These findings suggest that CXCL12 activates Runx2 and Osterix by activating Smads, thereby promoting MSCs differentiation into osteoblasts at early-stage. However, AMD3100 blocks the binding of CXCL12 to CXCR4 on the cell surface [32], leading to the decreased ability of MSCs to differentiate into osteoblasts. Thus, we infer that CXCL12 regulates the BMP-2/Smad/Runx2/Osterix axis by binding/dissociating with CXCR4 on the MSCs surface, thereby affecting their osteogenic differentiation. Simultaneously, we observed that Smad1/5/8, Runx2 and Osterix mRNA and protein expressions were not significantly diminished in the AMD3100 group compared with the control group. In the absence of CXCL12 overexpression, the CXCL12/CXCR4 axis did not significantly affect the early osteogenic differentiation of MSCs. Thus, blocking this signal axis cannot affect its osteogenic differentiation potential.

ALP is a representative marker of osteoblasts that directly reflects their activity and often serves as a marker of early osteogenic differentiation. One week after treatment, ALP activity was highest in the Ad-CXCL12 group; moreover, ALP activity was obviously lower in the Ad-CXCL12+AMD3100 group than in the Ad-CXCL12 group. These results further confirmed that CXCL12 could participate in early osteogenic differentiation by binding to CXCR4 on the MSCs surface. OPN is a regulator of matrix mineralization that is extensively expressed during early osteoblast differentiation through to mature osteocytes [33]. BSP is predominantly expressed in calcified tissue, acting as the initiation site of hydroxyapatite formation [34], and can promote preosteoblast differentiation into osteoblasts. OCN is an extracellular matrix protein that mainly arises during mineralization, so is considered a sign of osteoblast maturation [35]. As a result, all three markers were used to assess MSCs osteogenic differentiation. We found that after transfection with Ad-CXCL12, only BSP mRNA levels were obviously increased compared with the non-transfected group; whilst OCN and OPN mRNA expression levels were not increased. At 21 days, the number of mineralized nodules was observed in each group as a marker for late osteogenic differentiation. No significant differences in the numbers of mineralized nodules were observed among treatment groups, possibly because the extensively expressed CXCR4 in MSCs [36] is reported to noticeably reduce after cell differentiation [37]. In fact CXCL12 induced by dexamethasone has been shown to be highly expressed at early-stage, but diminish during cell differentiation [38]. During MSCs differentiation into preosteoblasts, osteoblasts and mature osteocytes, decreased CXCR4 and CXCL12 secretion leads to reduced CXCL12/CXCR4 axis involvement in the process of osteogenic differentiation. This explains why no significant effect of the altered CXCL12/CXCR4 axis was observed at mid- and late-stages of MSCs differentiation.

In summary, the CXCL12/CXCR4 axis promotes early osteogenic differentiation of MSCs by regulating the BMP-2/Smads/Runx2/Osterix axis, and mRNA expression of BSP, OCN and OPN. However, during MSCs differentiation into mature osteocytes, CXCL12 expression was gradually reduced and CXCR4 expression on the cell surface diminished. Interestingly, the CXCL12/CXCR4 axis had no significant effect on the mid- and late-stages of MSCs osteogenic differentiation. The CXCL12/CXCR4 axis is considered the main signal axis for MSCs migration [39, 40]. These findings suggest that crosstalk exists between the CXCL12-mediated migration signal axis and osteogenic signal axis, with cell-surface CXCR4 acting as the intersection. These findings provide a new way to solve the problems associated with the application of MSCs in the repair of necrotic bone tissue, such as the insufficient numbers of local MSCs and diminished osteogenic capacity of MSCs.

Acknowledgements

This study was supported by the National Natural Science Foundation of China (No.

81472103, 81071463); Key project of Natural Science Foundation of Hubei Province (No. 2015CFA079); the Applied Basic Research Project of Technology Bureau of Wuhan City of China (No. 2015061701011626); the "HuangheYingcai" Project of Wuhan City of China; the Wuhan Innovation Talent Development Foundation of Wuhan City of China; the Young and Middle-Aged Medical Personnel Training Project of Health and Family Planning Commission of Wuhan City of China.

Disclosure of conflict of interest

None.

Address correspondence to: Zhanghua Li, Tongren Hospital of Wuhan University, No. 216, Guanshan Road, Hongshan District, Wuhan 430074, Hubei Province, China. Tel: +86 18971610121; E-mail: lzh999999@aliyun.com

References

[1] Karp JM, Leng Teo GS. Mesenchymal stem cell homing: the devil is in the details. Cell Stem Cell 2009; 4: 206-216.

[2] Kocher AA, Schuster MD, Szabolcs MJ, Takuma S, Burkhoff D, Wang J, Homma S, Edwards NM, Itescu S. Neovascularization of ischemic myocardium by human bone-marrow-derived angioblasts prevents cardiomyocyte apoptosis, reduces remodeling and improves cardiac function. Nat Med 2001; 7: 430-436.

[3] Kinnaird T, Stabile E, Burnett MS, Lee CW, Barr S, Fuchs S, Epstein SE. Marrow-derived stromal cells express genes encoding a broad spectrum of arteriogenic cytokines and promote in vitro and in vivo arteriogenesis through paracrine mechanisms. Circ Res 2004; 94: 678-685.

[4] Xiao ZM, Jiang H, Zhan XL, Wu ZG, Zhang XL. Treatment of osteonecrosis of femoral head with BMSCs-seeded bio-derived bone materials combined with rhBMP-2 in rabbits. Chin J Traumatol 2008; 11: 165-170.

[5] Hu X, Wei L, Taylor TM, Wei J, Zhou X, Wang JA, Yu SP. Hypoxic preconditioning enhances bone marrow mesenchymal stem cell migration via Kv2.1 channel and FAK activation. Am J Physiol Cell Physiol 2011; 301: C362-372.

[6] Huang YC, Zhu HM, Cai JQ, Huang YZ, Xu J, Zhou Y, Chen XH, Li XQ, Yang ZM, Deng L. Hypoxia inhibits the spontaneous calcification of bone marrow-derived mesenchymal stem cells. J Cell Biochem 2012; 113: 1407-1415.

[7] Wang Y, Li J, Wang Y, Lei L, Jiang C, An S, Zhan Y, Cheng Q, Zhao Z, Wang J, Jiang L. Effects of hypoxia on osteogenic differentiation of rat bone marrow mesenchymal stem cells. Mol Cell Biochem 2012; 362: 25-33.

[8] Fox JM, Chamberlain G, Ashton BA, Middleton J. Recent advances into the understanding of mesenchymal stem cell trafficking. Br J Haematol 2007; 137: 491-502.

[9] Marquez-Curtis LA, Janowska-Wieczorek A. Enhancing the migration ability of mesenchymal stromal cells by targeting the SDF-1/CXCR4 axis. Biomed Res Int 2013; 2013: 561098.

[10] Li Q, Guo Y, Chen F, Liu J, Jin P. Stromal cell-derived factor-1 promotes human adipose tissue-derived stem cell survival and chronic wound healing. Exp Ther Med 2016; 12: 45-50.

[11] Kanbe K, Chiba J, Inoue Y, Taguchi M, Yabuki A. SDF-1 and CXCR4 in synovium are associated with disease activity and bone and joint destruction in patients with rheumatoid arthritis treated with golimumab. Mod Rheumatol 2016; 26: 46-50.

[12] Sauvé K, Lepage J, Sanchez M, Heveker N, Tremblay A. Positive feedback activation of estrogen receptors by the CXCL12-CXCR4 pathway. Cancer Res 2009; 69: 5793-5800.

[13] Zhang W, Yuan Z, Pei X, Ma R. In vivo and in vitro characteristic of HIF-1α and relative genes in ischemic femoral head necrosis. Int J Clin Exp Pathol 2015; 8: 7210-7216.

[14] Youn SW, Lee SW, Lee J, Jeong HK, Suh JW, Yoon CH, Kang HJ, Kim HZ, Koh GY, Oh BH, Park YB, Kim HS. COMP-Ang1 stimulates HIF-1α-mediated SDF-1 overexpression and recovers ischemic injury through BM-derived progenitor cell recruitment. Blood 2011; 117: 4376-4386.

[15] Grunewald M, Avraham I, Dor Y, Bachar-Lustig E, Itin A, Jung S, Chimenti S, Landsman L, Abramovitch R, Keshet E. VEGF-induced adult neovascularization: recruitment, retention, and role of accessory cells. Cell 2006; 124: 175-189.

[16] Hosogane N, Huang Z, Rawlins BA, Liu X, Boachie-Adjei O, Boskey AL, Zhu W. Stromal derived factor-1 regulates bone morphogenetic protein 2-induced osteogenic differentiation of primary mesenchymal stem cells. Int J Biochem Cell Biol 2010; 42: 1132-1141.

[17] Zhu W, Boachie-Adjei O, Rawlins BA, Frenkel B, Boskey AL, Ivashkiv LB, Blobel CP. A novel regulatory role for stromal-derived factor-1 signaling in bone morphogenic protein-2 osteogenic differentiation of mesenchymal C2C12 cells. J Biol Chem 2007; 282: 18676-18685.

[18] Shirozu M, Nakano T, Inazawa J, Tashiro K, Tada H, Shinohara T, Honjo T. Structure and chromosomal localization of the human stro-

mal cell-derived factor 1 (SDF1) gene. Genomics 1995; 28: 495-500.
[19] Kowalski K, Archacki R, Archacka K, Stremińska W, Paciorek A, Gołąbek M, Ciemerych MA, Brzoska E. Stromal derived factor-1 and granulocyte-colony stimulating factor treatment improves regeneration of Pax7-/- mice skeletal muscles. J Cachexia Sarcopenia Muscle 2016; 7: 483-496.
[20] Ohnishi H, Mizuno S, Mizuno-Horikawa Y, Kato T. Stromal cell-derived factor-1 (SDF1)-dependent recruitment of bone marrow-derived renal endothelium-like cells in a mouse model of acute kidney injury. J Vet Med Sci 2015; 77: 313-319.
[21] Lin HH, Chen YH, Chiang MT, Huang PL, Chau LY. Activator protein-2α mediates carbon monoxide-induced stromal cell-derived factor-1α expression and vascularization in ischemic heart. Arterioscler Thromb Vasc Biol 2013; 33: 785-794.
[22] DeLeve LD, Wang X, Wang L. VEGF-sdf1 recruitment of CXCR7+ bone marrow progenitors of liver sinusoidal endothelial cells promotes rat liver regeneration. Am J Physiol Gastrointest Liver Physiol 2016; 310: G739-746.
[23] Liu H, Li M, Du L, Yang P, Ge S. Local administration of stromal cell-derived factor-1 promotes stem cell recruitment and bone regeneration in a rat periodontal bone defect model. Mater Sci Eng C Mater Biol Appl 2015; 53: 83-94.
[24] Chen G, Fang T, Qi Y, Huang Z, Du S, Di T, Feng G, Lei Z, Zhang Y, Yan W. Combined use of mesenchymal stromal cell sheet transplantation and local injection of SDF-1 for bone repair in a rat non-union model. Cell Transplant 2016; [Epub ahead of print].
[25] Zhang SJ, Song XY, He M, Yu SB. Effect of TGF-β1/SDF-1/CXCR4 signal on BM-MSCs homing in rat heart of ischemia/perfusion injury. Eur Rev Med Pharmacol Sci 2016; 20: 899-905.
[26] Abduelmula A, Huang R, Pu Q, Tamamura H, Morosan-Puopolo G, Brand-Saberi B. SDF-1 controls the muscle and blood vessel formation of the somite. Int J Dev Biol 2016; 60: 29-38.
[27] Zhang JF, Fu WM, He ML, Xie WD, Lv Q, Wan G, Li G, Wang H, Lu G, Hu X, Jiang S, Li JN, Lin MC, Zhang YO, Kung HF. MiRNA-20a promotes osteogenic differentiation of human mesenchymal stem cells by co-regulating BMP signaling. RNA Biol 2011; 8: 829-838.
[28] Zhang X, Aubin JE, Inman RD. Molecular and cellular biology of new bone formation: insights into the ankylosis of ankylosing spondylitis. Curr Opin Rheumatol 2003; 15: 387-393.
[29] Maruyama Z, Yoshida CA, Furuichi T, Amizuka N, Ito M, Fukuyama R, Miyazaki T, Kitaura H, Nakamura K, Fujita T, Kanatani N, Moriishi T, Yamana K, Liu W, Kawaguchi H, Nakamura K, Komori T. Runx2 determines bone maturity and turnover rate in postnatal bone development and is involved in bone loss in estrogen deficiency. Dev Dyn 2007; 236: 1876-1890.
[30] Li ZH, Liao W, Cui XL, Chen YH, Liu TS, Liu M, Yang Y. Effects of Cbfa1 on osteoanagenesis during avascular necrosis of femoral head. Scientific Research & Essays 2010; 5: 2721-2730.
[31] Ohyama Y, Nifuji A, Maeda Y, Amagasa T, Noda M. Spaciotemporal association and bone morphogenetic protein regulation of sclerostin and osterix expression during embryonic osteogenesis. Endocrinology 2004; 145: 4685-4692.
[32] Hatse S, Princen K, Bridger G, De Clercq E, Schols D. Chemokine receptor inhibition by AMD3100 is strictly confined to CXCR4. FEBS Lett 2002; 527: 255-2562.
[33] Sodek J, Ganss B, McKee MD. Osteopontin. Crit Rev Oral Biol Med 2000; 11: 279-303.
[34] Saito Y, Yoshizawa T, Takizawa F, Ikegame M, Ishibashi O, Okuda K, Hara K, Ishibashi K, Obinata M, Kawashima H. A cell line with characteristics of the periodontal ligament fibroblasts is negatively regulated for mineralization and Runx2/Cbfa1/Osf2 activity, part of which can be overcome by bone morphogenetic protein-2. J Cell Sci 2002; 115: 4191-4200.
[35] Fujisawa R, Tamura M. Acidic bone matrix proteins and their roles in calcification. Front Biosci (Landmark Ed) 2012; 17: 1891-1903.
[36] Kitaori T, Ito H, Schwarz EM, Tsutsumi R, Yoshitomi H, Oishi S, Nakano M, Fujii N, Nagasawa T, Nakamura T. Stromal cell-derived factor 1/CXCR4 signaling is critical for the recruitment of mesenchymal stem cells to the fracture site during skeletal repair in a mouse model. Arthritis Rheum 2009; 60: 813-823.
[37] Kortesidis A, Zannettino A, Isenmann S, Shi S, Lapidot T, Gronthos S. Stromal-derived factor-1 promotes the growth, survival, and development of human bone marrow stromal stem cells. Blood 2005; 105: 3793-3801.
[38] Ratajczak MZ, Majka M, Kucia M, Drukala J, Pietrzkowski Z, Peiper S, Janowska-Wieczorek A. Expression of functional CXCR4 by muscle satellite cells and secretion of SDF-1 by muscle-derived fibroblasts is associated with the presence of both muscle progenitors in bone marrow and hematopoietic stem/progenitor cells in muscles. Stem Cells 2003; 21: 363-371.
[39] Liu X, Duan B, Cheng Z, Jia X, Mao L, Fu H, Che Y, Ou L, Liu L, Kong D. SDF-1/CXCR4 axis modulates bone marrow mesenchymal stem cell

apoptosis, migration and cytokine secretion. Protein Cell 2011; 2: 845-854.

[40] Li L, Wu S, Liu Z, Zhuo Z, Tan K, Xia H, Zhuo L, Deng X, Gao Y, Xu Y. Ultrasound-targeted microbubble destruction improves the migration and homing of mesenchymal stem cells after myocardial infarction by upregulating SDF-1/CXCR4: a pilot study. Stem Cells Int 2015; 2015: 691310.